# Rates and populations of compact binary mergers

## *Caltech LIGO SURF 2019, First Interim Report*

Phoebe McClincy (phoebemcclincy@gmail.com)
*Department of Astronomy and Astrophysics, Pennsylvania State University*

**Mentors:** Alan Weinstein, Jonah Kanner, Liting Xiao
*LIGO Laboratory, California Institute of Technology*
(Dated: 10 July 2019)

The LIGO and Virgo detectors have been observing the cosmos in search of gravitational waves (GW) since 2000. All three detectors were upgraded to Advanced versions, which for LIGO began observing in 2015 and for Virgo in 2017. In Advanced LIGO's first (12 September 2015 to 19 January 2016) and second (30 November 2016 to 25 August 2017) observing runs (O1 and O2, respectively), the detectors found 10 GW signals from binary black hole (BBH) mergers, and 1 from a binary neutron star (BNS) merger, all with high significance, or low probability of being due to instrumental noise fluctuations. Already in the first several months of O3, which began in April 2019, 2 BNS signals, 15 BBH signals, and 1 NSBH candidate have been seen with such high significance. These three categories are collectively known as compact binary coalescence (CBC). In the coming years, as the detectors' sensitivities are improved, we expect to accumulate tens, hundreds, or thousands of CBC events. From such large samples, we expect to be able to infer the underlying population of CBC systems as a function of their masses, component black hole spins, and redshift. This, in turn, will allow us to better understand the astrophysical processes governing the formation, evolution, and final fate of such systems, as tracers of the most massive stars. In this project, we aim to develop tools and techniques to accomplish this through detailed simulation and Bayesian inference. *We report the first three weeks of progress during this project.*

## I. MOTIVATIONS

### A. Measuring binaries with gravitational waves

Gravitational radiation results in the distortion of spacetime between matter. Thus, when a GW propagates through Earth, it causes a change in the distance between objects to occur. This quantity is known as strain, which is observed in the arms of our detectors. Strain, in terms of what the observer sees, is described by

$$h = \frac{\Delta L}{L}, \tag{1}$$

where $L$ is the original length of the detector arm, and $\Delta L$ is the change in that length as induced by a GW.

It is known from general relativity that strain is determined by a binary's parameters. Strain depends primarily on the intrinsic parameters, mass and spin, which directly affect the shape of the observed waveform. The other parameters, which are all observer-dependent, govern only the strength of the signal. We can thus analyze the evolution of the waveform's shape by using Bayesian inference techniques to determine the chirp mass $\mathcal{M}$, and subsequently the symmetric mass ratio $\eta$. The component masses are implicit in $\eta$ [1]:

$$\eta = \frac{m_1 m_2}{M_{tot}^2} = (\frac{\mathcal{M}}{M_{tot}})^{\frac{5}{3}}. \tag{2}$$

The ultimate goal of this project is to learn about the universe's more massive stars, which lead to the formation of BBH. It is strongly believed that the component masses of a BBH are related to the masses of its progenitor stars. More massive stars, such as those that form BBH, have lower metallicity and were formed early in the universe's timeline (before heavier elements existed). Younger, higher-metallicity stars have masses too small to form BBH; as such, it is important to determine the underlying distribution of the high-mass progenitor stars so that we may be informed about their evolution into BBH.

At present, there exist well-supported models of the star formation rate as a function of redshift ($z$). These models are based on observations from electromagnetic radiation [2, 3]. For BH, we postulate a relation between BH event rate density $\mathcal{R}$, $z$, and mass. We describe $\mathcal{R}$, or the number of events per unit comoving volume per unit time, as

$$\mathcal{R} = \frac{dN}{dV_c dt_s}. \tag{3}$$

We aim to determine the dependence of $\mathcal{R}$ on $z$, and the underlying distribution of high masses that accompanies such a relation. Upon determining the underlying mass distribution, we are equipped to establish a link between the stellar mass function and the BBH mass function.

Although there are six parameters used to describe spin, only two combinations of them dominate in the phase and amplitude evolution of a gravitational wave-

form: the effective spin of the orbit, $\chi_{\rm eff}$, and the precessional spin of the orbit, $\chi_{\rm p}$. $\chi_{\rm eff}$ is simply the combination of the component spins along the binary's orbital angular momentum vector [4]. $\chi_{\rm p}$, however, governs the precession of the binary's orbital plane. These quantities carry information about the mechanisms by which a binary was formed, and are described [5] by

$$\chi_{\rm eff} = \frac{a_1 m_1 \cos\theta_1 + a_2 m_2 \cos\theta_2}{m_1 + m_2}, \tag{4}$$

and

$$\chi_{\rm p} = \max\big(a_1 \sin\theta_1, (\frac{4m_1 + 3m_2}{4m_2 + 3m_1})(\frac{m_1}{m_2}) a_2 \sin\theta_2\big), \tag{5}$$

where $\theta_1$ and $\theta_2$ are the angles between the angular momentum vectors of each component and the binary's total angular momentum vector.

Because spin is a higher-order effect in gravitational waveform evolution, it is more difficult to measure, whereas mass is of first-order and its range of values can be more accurately constrained. As such, we will primarily focus on mass for now.

### B. Channels of formation

If we are able to determine the underlying distribution of masses, we are then able to gain valuable insights into possible methods by which a binary in question was formed. There are many proposed formation channels, but two (shown in Fig. 1) that are of particular interest to us [6]. The first main channel is common evolution. In one common evolution sub-channel marked by a common envelope phase, the BBH evolves via traditional collapse of both components from a progenitor stellar binary, within a single cloud of gas. In another sub-channel, the BBH forms via chemically homogeneous evolution, in which the orbit of the binary components does not expand traditionally during main sequence helium production, but rather remains compact [7].

The second main channel is dynamical formation, which entails the interaction of components formed independently of each other. In one such case, a binary system interacts with a third body in a dense stellar cluster, which results in the ejection of the binary's less massive component and the capture of the third, more massive body into the binary. In another dynamical formation case, one single body captures a second body via the Bremsstrahlung radiation caused by the acceleration of the second body through the first body's gravitational field. We aim to be able to distinguish between these formation channels, primarily from mass, then eventually from spin.

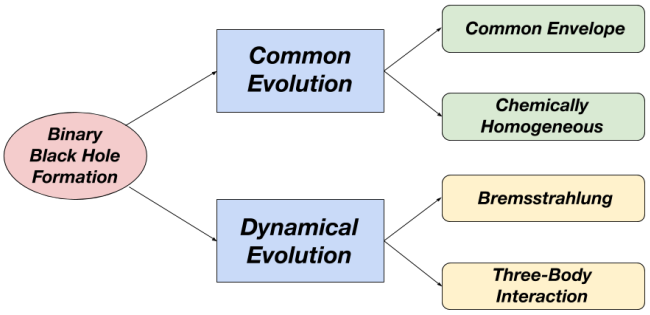


FIG. 1. Formation channels of interest for binary black holes. The first such channel is common evolution, in which binaries are either formed from common envelope evolution or chemically-homogeneous evolution. The second such channel is dynamical formation, in which black holes formed in separate environments interact, in either two-body or three-body interactions.

### C. Populations, mass distributions, and mass gaps

Within the mass distribution of CBC events (shown in Fig. 2), there exist three proposed regions of scarcity (mass gaps): one below 1 $M_\odot$, one between ∼2-5 $M_\odot$, and another between ∼50-150 $M_\odot$. The latter is proposed to exist due to pulsational pair-instability supernovae [8], in which progenitor binary stars with component masses between 100-150 $M_\odot$ eject a significant amount of their mass upon going supernova. This theoretically causes the subsequent BBH component masses to settle around ∼40 $M_\odot$ [9]. We can thus infer truths about this particular mass gap by determining the underlying mass distribution of BBH.

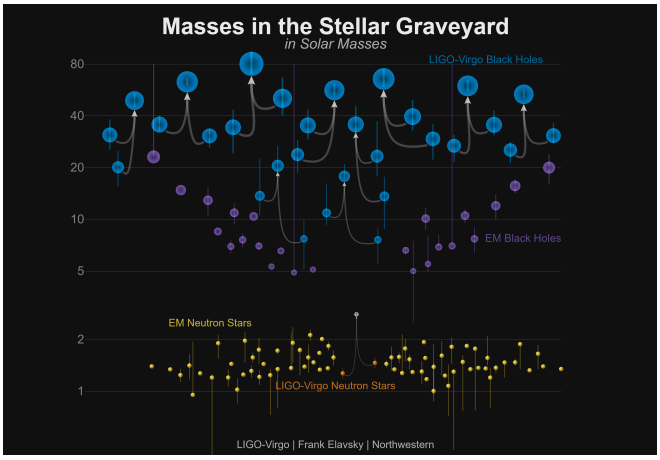


FIG. 2. Distribution of NS and BH masses, as detected via electromagnetic radiation and Advanced LIGO. There are regions of scarcity below 1 $M_\odot$ and between ∼2-5 $M_\odot$, as well as a possible mass gap between ∼50-150 $M_\odot$.

## II. PROJECT

At present, LIGO has catalogued 29 CBC events, 18 of which have been detected solely in the third observing run. As our detectors improve, the volume of spacetime in which LIGO is able to observe increases. This quantity is known as the sensitive spacetime volume

$$\langle VT \rangle = \frac{4}{3}\pi D_{avg}^3 T, \tag{6}$$

where $D_{avg}$ represents LIGO's sensitive distance and $T$ represents the observation time of the LIGO detectors [10]. It is important to note that $D_{avg}$ is a strong function of mass; systems with a larger overall mass produce louder GW, and result in a larger $D_{avg}$. Because $\langle VT \rangle$ is proportional to the sensitivity of our detectors, we are able to observe larger regions of spacetime as we produce higher-quality detectors.

As larger regions of spacetime are observed, LIGO is expected to recover events in larger and larger numbers. A larger sample size of BBH offers the unique opportunity to reveal the underlying naturally-occurring distributions of and relations between BBH masses, spins, merger rates, and redshift, among other parameters. By studying populations of BBH, we may better understand the relationship between the progenitor star initial mass function and the mass function that governs BBH. We also stand to uncover information about which formation channel is more prevalent in nature, as well as the hyperparameters we would expect each formation channel to follow. We plan to carry out detailed simulation and Bayesian inference to do so.

The actual amount of events that we have observed (or our collected data) is described as $N$. The true number of events that occur in nature is described as

$$\hat{N}_{true} = \int \frac{dN}{dm_1 dm_2 dz dt_s} dm_1 dm_2 dz dt_s. \tag{7}$$

The component masses $m_1$ and $m_2$, as well as source time $t_s$ and $z$, can be written as a series of parameters called $\vec{\theta}$. We assume that $\hat{N}_{true}$ depends on $m_1$ and $m_2$, the distribution of which we will describe by hyperparameters $\alpha$ and $\beta$, respectively. We also assume that $\mathcal{R}$ has a dependence on $z$, which is described by another hyperparameter $\gamma$. Collectively, we denote these hyperparamters $\vec{\lambda}$. Spin is also believed to be a dependent of $\hat{N}_{true}$; however, we will not address spin at this point in the project. We can thus rewrite Eqn. (7) as

$$\hat{N}_{true} = \int \frac{dN(\lambda)}{d\vec{\theta}} d\vec{\theta}, \tag{8}$$

where

$$\frac{dN(\lambda)}{d\vec{\theta}} = \mathcal{R}(1+z)^{\gamma} f(m_1|\alpha) f(m_2|\beta) \frac{dV_c}{dz} \frac{dt_d}{dt_s} \frac{1}{T_d}, \tag{9}$$

with $t_d$ being the time as measured at the detector (which has been dilated with respect to the time at the source), $T_d$ the observation time of the detector, and $V_c$ the comoving volume, whose relation to $z$ is determined in accordance with the ΛCDM cosmological model [11]. From this, we can construct an expression for the expected amount of events that we will observe:

$$\hat{N}_{det} = \int \frac{dN(\lambda)}{d\vec{\theta}} \mathcal{E}(\vec{\theta}) d\vec{\theta}, \tag{10}$$

where $\mathcal{E}(\vec{\theta})$ represents the efficiency of detection. Upon collecting $N$, we can construct a Poissonian probability distribution for $N$ such that

$$P(N|\hat{N}_{det}, \lambda) = \frac{\hat{N}_{det}^N e^{-\hat{N}_{det}}}{N!}. \tag{11}$$

However, we are looking to infer what the true, naturally-occurring number of events is; thus, we step through this process in the reverse.

To do this, we plan to randomly generate a population of masses and propose possible values for the hyperparameters enveloped in $\vec{\lambda}$. We will develop methodology for measuring $\vec{\lambda}$ using Bayesian inference to compare how close our experimentally-recovered values are to our proposed values. In particular, we will use the dynamic nested sampler dynesty [12] to carry this process out. Simply put, we will do this in three major steps:

(1) Simulate a dataset consisting of many observed binary systems, following the distribution outlined in Eqn. (9) with an arbitrary choice of $\vec{\lambda}$.

(2) Use Bayesian inference techniques to recover the most accurate posterior probability distribution for the underlying $\vec{\lambda}$.

(3) Reconstruct the distribution for $\hat{N}_{true}$.

This has been attempted by other groups. In [13], three models were presented for the BBH primary mass distribution, denoted Models A, B, and C. Model A fixes $m_{min}$ to be 5 $M_{\odot}$, and allows $m_{max}$ to vary. Model B allows both mass limits to vary. Model C allows multiple functions to describe the distribution; a second component of Gaussian nature appears due to the pair instability in massive progenitor stars. As such, for Model C, a power law distribution fits at lower masses, and a Gaussian distribution fits at higher masses. We plan to use Model C as a starting point for the analysis done in this project.

## III. PROGRESS

Thus far, I have worked on laying the foundations for beginning the analysis within this project. I have worked on generating my own distributions and conducting parameter estimation on them. My warm-up assignment was to generate a distribution of masses that followed a

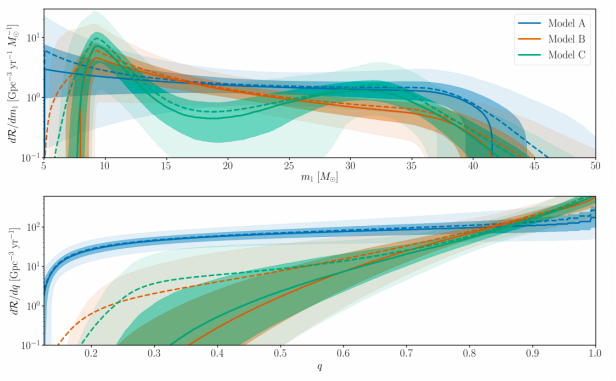


FIG. 3. Differential merger rate distribution for BBH as a function of primary mass and mass ratio ($q$) for proposed Models A, B, and C in [13]. At lower masses, Model C follows a power law distribution, and at higher masses, it follows a Gaussian distribution. This distribution is based on data from O1 and O2 only (10 BBH mergers); we plan to begin our testing using this model.

power law (in particular, the Salpeter Initial Mass Function (IMF), $N = M^{-2.35}$). I did this using 50 randomly-generated points governed by Gaussian distributions with standard deviations of 0.002, shown in Fig. 4.

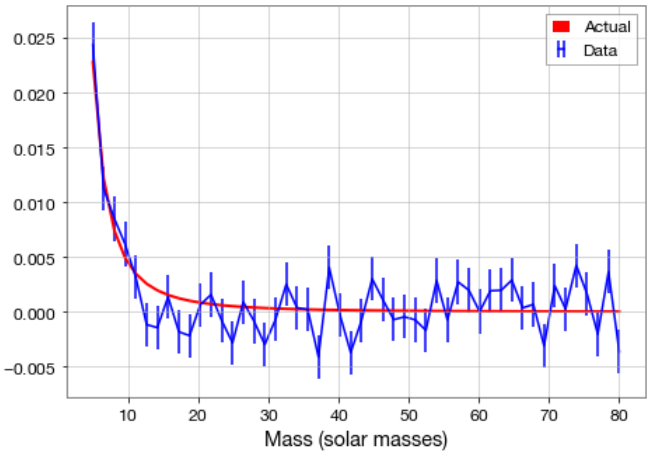


FIG. 4. Results from the initial random generation of masses following the Salpeter IMF; the red curve is the actual distribution, whereas the blue curve represents the 50 generated points and their Poisson errors.

I then used dynesty for parameter estimation, and generated posterior distributions for both hyperparameters of the power law, the amplitude and power law slope. Overall, the true values and the data values were consistent, as shown in Fig. 5.

I then repeated this process using a different method called the Inverse Transform Method (ITM), which entails using the inverse cumulative density function (CDF) to sample the original distribution. This is done by generating numbers selected from a uniform distribution between 0 and 1, and transforming them into points on the

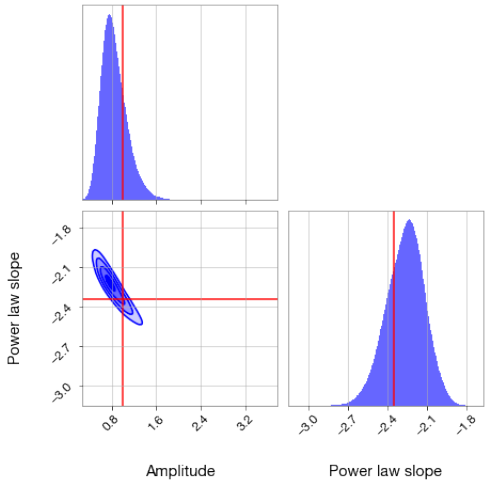


FIG. 5. Posterior distributions for amplitude and power law slope as generated by dynesty, along with the parameters' correlation.

original distribution using the inverse CDF.

Next, I will begin to construct a program which carries out the first process for a more complicated distribution of masses, governed by the aforementioned Model C.

## IV. CHALLENGES AND FUTURE PROSPECTS

So far, the main sources of my challenges have been figuring out how to use dynesty and using the ITM. At first, I had trouble understanding exactly what dynesty was used for and how it tied into the work I would be doing. Over the past three weeks, I have been able to use dynesty to complete the warm-up exercise and have learned a lot about Bayesian inference, which has aided in my understanding of dynesty's use. In regards to the ITM, I carried out the process both analytically and numerically. I spent a day working on it analytically (and attempting to solve an unsolvable math problem) before realizing that I was working with the entirely wrong function. However, once I was using the correct function, I was able to complete the exercise with no problems.

In the future, I anticipate having more trouble with dynesty. I am still learning more about Bayesian inference and dynesty's applications, so as I learn more, I hope it will become easier to use. The first distribution that we will be analyzing has multiple functions within one distribution, so I anticipate it will be a challenge to write the proper code to analyze it, since I have only worked with simpler functions thus far.

[1] B. S. Sathyaprakash and B. F. Schutz, "Physics, astrophysics and cosmology with gravitational waves," *Living reviews in relativity*, vol. 12, no. 1, p. 2, 2009.

[2] A. E. Bauer, N. Drory, G. Hill, and G. Feulner, "Specific star formation rates to redshift 1.5," *The Astrophysical Journal Letters*, vol. 621, no. 2, p. L89, 2005.

[3] F. Mannucci, G. Cresci, R. Maiolino, A. Marconi, and A. Gnerucci, "A fundamental relation between mass, star formation rate and metallicity in local and high-redshift galaxies," *Monthly Notices of the Royal Astronomical Society*, vol. 408, no. 4, pp. 2115–2127, 2010.

[4] K. K. Ng, S. Vitale, A. Zimmerman, K. Chatziioannou, D. Gerosa, and C.-J. Haster, "Gravitational-wave astrophysics with effective-spin measurements: Asymmetries and selection biases," *Physical Review D*, vol. 98, no. 8, p. 083007, 2018.

[5] C. Talbot and E. Thrane, "Determining the population properties of spinning black holes," *Physical Review D*, vol. 96, no. 2, p. 023012, 2017.

[6] C. L. Rodriguez, M. Zevin, C. Pankow, V. Kalogera, and F. A. Rasio, "Illuminating black hole binary formation channels with spins in advanced ligo," *The Astrophysical Journal Letters*, vol. 832, p. L2, 2016.

[7] S. de Mink, M. Cantiello, N. Langer, and O. Pols, "Chemically homogeneous evolution in massive binaries," in *AIP Conference Proceedings*, vol. 1314, pp. 291–296, AIP, 2010.

[8] C. Fryer, S. Woosley, and A. Heger, "Pair-instability supernovae, gravity waves, and gamma-ray transients," *The Astrophysical Journal*, vol. 550, p. 372, 2001.

[9] C. Talbot and E. Thrane, "Measuring the binary black hole mass spectrum with an astrophysically motivated parameterization," *The Astrophysical Journal*, vol. 856, p. 173, 2018.

[10] R. Magee, A.-S. Deutsch, P. McClincy, C. Hanna, C. Horst, D. Meacher, C. Messick, S. Shandera, and M. Wade, "Methods for the detection of gravitational waves from subsolar mass ultracompact binaries," *Physical Review D*, vol. 98, no. 10, p. 103024, 2018.

[11] D. W. Hogg, "Distance measures in cosmology," *arXiv preprint astro-ph/9905116*, 1999.

[12] J. S. Speagle, "dynesty: A dynamic nested sampling package for estimating bayesian posteriors and evidences," *arXiv preprint arXiv:1904.02180*, 2019.

[13] B. Abbott, R. Abbott, T. Abbott, S. Abraham, F. Acernese, K. Ackley, C. Adams, R. Adhikari, V. Adya, C. Affeldt, *et al.*, "Binary black hole population properties inferred from the first and second observing runs of advanced ligo and advanced virgo," *arXiv preprint arXiv:1811.12940*, 2019.